

## Article

# Synthesis of Multicomponent Coatings by Electrosark Alloying with Powder Materials

Valentin Mihailov <sup>1,\*</sup>, Natalia Kazak <sup>1</sup>, Sergiu Ivashcu <sup>1</sup>, Evgenii Ovchinnikov <sup>2</sup>, Constantin Baciuc <sup>3</sup>, Anatoli Ianachevici <sup>1</sup>, Raimundas Rukuiza <sup>4</sup>  and Audrius Zunda <sup>3,\*</sup>

<sup>1</sup> Institute of Applied Physics, 2028 Chisinau, Moldova

<sup>2</sup> Grodno State University Named after Yanki Kupaly, 230023 Grodno, Belarus

<sup>3</sup> Department of Materials Engineering and Industrial Security, "Gh. Asachi" Technical University of Iasi, 700050 Iasi, Romania

<sup>4</sup> Agriculture Academy, Vytautas Magnus University, 53361 Kaunas, Lithuania

\* Correspondence: valentin.mihailov@gmail.com (V.M.); audrius.zunda@vdu.lt (A.Z.)

**Abstract:** The results of systematic studies of the electrosark alloying process with the introduction of dispersed materials into plasma of low-voltage pulsed discharges are presented. Technological methods have been developed for supplying the powder material straight into the treatment zone through a hollow electrode of an anode or from the side, with the electrode-anode periodically contacting the substrate of cathode. It has been established that under the same energy regimes, when powder materials were introduced into the discharge zone, the increase in the mass of the cathode per time unit increases from 10 to 15 times or more. This study presents the process of synthesis of carbide phases (TiC and WC) during electrosark alloying of steel substrates with electrodes made of Ti, W, and graphite, with additional supply powders of these materials into the processing zone. A process has been developed for the synthesis of ternary compounds, so-called MAX-phases: Ti<sub>2</sub>AlC, Ti<sub>2</sub>AlN and Ti<sub>3</sub>SiC<sub>2</sub> by electrosark alloying with powder compositions TiAlC, TiAlN and TiSiC. These MAX phases exhibit a unique combination of properties that are characteristic of both metals and ceramics. Energy modes of the processing were optimized, which resulted in high-quality coatings with the maximum content of carbide phases and ternary compounds. It has been established that the energy of electrical pulses during electrosark alloying, when powders of materials are fed into the interelectrode gap, ranges from 0.8 to 3.0 J, depending on their thermal physical properties. High wear and corrosion resistant characteristics of C45 structural steel with such electrosark coatings are obtained. The wear of steel with coatings in comparison with uncoated steel decreased by an average of 5.5–6.0 times. It was estimated the high corrosion resistance of 40X13 steel coated with TiC and WC in 3% NaCl solution. The corrosion current for these coatings is 0.044 and 0.075 A/cm<sup>2</sup>, respectively, and is significantly less than for coatings made of TiAlC, TiAlN, and TiSiC compositions. X-ray phase and optical metallographic microscopy analyses enabled the display of the amorphous-crystalline nature of the coatings.

**Keywords:** electrosark alloying; powder materials; MAX-phases; multicomponent coatings



**Citation:** Mihailov, V.; Kazak, N.; Ivashcu, S.; Ovchinnikov, E.; Baciuc, C.; Ianachevici, A.; Rukuiza, R.; Zunda, A. Synthesis of Multicomponent Coatings by Electrosark Alloying with Powder Materials. *Coatings* **2023**, *13*, 651. <https://doi.org/10.3390/coatings13030651>

Academic Editor: Salvatore Grasso

Received: 31 January 2023

Revised: 8 March 2023

Accepted: 10 March 2023

Published: 20 March 2023



**Copyright:** © 2023 by the authors. Licensee MDPI, Basel, Switzerland. This article is an open access article distributed under the terms and conditions of the Creative Commons Attribution (CC BY) license (<https://creativecommons.org/licenses/by/4.0/>).

## 1. Introduction

Electrophysical materials processing methods based on the use of concentrated energy flows, such as electron and laser beams, low-temperature plasma, pulsed discharges, and the others, are very promising for surface hardening and applying protective coatings [1]. Electrosark alloying (ESA) of metal surfaces is one of these methods. The method is based on the phenomenon of electrical erosion and transfer of the material of the anode (tool) to the cathode (substrate) during the flow of pulsed discharges in a gaseous medium. It was developed simultaneously with the method of electro-erosive machining [2]. In the case of electro-erosive machining, usually carried out in a dielectric liquid, part of the substrate

material is removed due to electrical erosion. By applying the electrospark alloying, carried out in a gaseous medium, the eroded material of the anode tool is transferred and deposited on the surface of the cathode substrate, resulting in the saturation (alloying) of the surface layer of the cathode with elements that are part of the anode material.

The main features of electrospark alloying include: the local surface treatment when the alloying can be carried out in strictly specified places without protecting the rest of the surface of the workpiece; high adhesion of the applied material to the substrate; the absence of detail overheating during the processing; the possibility to use as processing materials both pure and their alloys, refractory metal compounds, etc.; the diffusion saturation of the cathode surface with constituent elements of the anode without changing the dimensions of the cathode, i.e., detail. The technology of electrospark alloying is very simple, and the necessary equipment can be small-sized, reliable, and transportable. It is also important to note the very low energy consumption of the process compared to traditional processing methods, such as electric overlaying, electric arc metallization, plasma spraying, etc. [3,4].

In the traditional electrospark alloying process, for periodic excitation of discharges between the electrodes, the compact electrodes in the form of bars are vibrated with a frequency of 100 Hz or more or rotated at 600–800 rpm. Standard compact electrodes are obtained on the basis of the carbides of IV–VI group transition metals of the periodic system and are used mainly to increase the hardness of the working surfaces of machine parts and, consequently, to increase their service life [5–9]. The most common standardized electrodes, T15K6 (79%WC + 15%TiC + 6%Co), BK6 (94%WC + 6%Co) and BK8 (92% WC + 8%Co), are obtained from titanium carbides (TiC) and tungsten (WC) [10].

The mechanism of coating formation during processing with compact electrodes should be considered. As a result of periodic contact with the cathode surface, electrical discharges occur, causing erosion of the anode and the transfer of this eroded mass in the form of vapor and liquid phases to the cathode surface. The transferred anode material in the form of vapor and liquid phases interacts with the cathode material and forms the various chemical compounds, alloys, oxides, and nitrides, if the treatment is carried out in air. The intensity of anode erosion, the transfer of its material to the cathode, and the formation of a coating layer depend mainly on the magnitude of the pulsed discharge energy and the nature of the material. Previous studies and practical experience show that, despite a number of advantages of the ESA method with compact electrodes, its capabilities are often limited due to the low productivity of the process and thickness of the formed layers [11,12]. It is difficult to obtain high-quality coatings of these materials with a thickness greater than 0.1–0.15 mm. The main reason for that is the high erosion resistance of electrodes based on the carbides. The materials that are used to produce electrodes—refractory carbides—have high erosion resistance, and therefore, the amount of anode material transferred to the cathode at one discharge cycle is extremely small. These limitations and the low productivity of the process do not meet the requirements of modern industries for hardening technologies.

Our preliminary investigations with Ti, W, and the graphite as a carbon source as the standard components of the electrodes showed better results [6]. The layers with a high content of carbide phases were obtained, which caused the higher hardness of the treated surface. However, despite the availability of electrode materials and the reduction in the overall cost of the process, significant progress in increasing the productivity and thickness of the deposited layers has not been achieved.

It should be noted that in recent years, a significant number of studies have appeared where the authors use the method of electrospark alloying to increase the wear resistance of machine parts [7–9,12,13]. However, in these works, the ESA method is used only as a tool for solving their specific problems, and not a single work raises the question of its modernization. One of the ways to solve the problem of the development and modernization of the ESA method is to study the physical aspects that occur in the gap between the electrodes at the moment when the material particle enters it, and an electric pulsed discharge occurs.

In this regard, the authors of this investigation carried out systematic studies of the ESA process, with the simultaneous introduction of powder materials into the inter-electrode gap [11]. It was noticed that when a powder particle enters the inter-electrode gap, the discharge occurs at distances greater than discharge initiation distances. In this case, in the system, an anode/interelectrode gap/cathode takes place to redistribute thermal energy. As a result, the main regularities of coating formation were established, and the optimal values of the energy and technological parameters of the process were determined when the high-quality coatings could be obtained. The advantages of a new version of the electrospark alloying process were proven, which significantly increased the productivity of coating formation, its thickness, and hence the service life. One of the main advantages of such an electrospark alloying process with powder materials is a significant expansion of the range of materials used as alloying elements and the possibility to obtain multicomponent coatings and control their properties.

## 2. Materials and Methods

To conduct research, a number of experimental pulse generator models were used, which work in a wide range of electrical pulse energy values, their repetition rate, and operating current.

Compact electrodes made of transition metals (Ti, Ta, W) were used as alloying materials, graphite electrodes as a source of carbon, as well as their powders and mixtures of powders of various compounds. The compact electrodes in the form of rectangular bars measuring  $35 \times 5 \times 5$  mm in size, as well as cylindrical bars measuring 5 mm in diameter and 35–40 mm long were used.

The grain size of the powders was chosen depending on the conditions of good fluidity from the supply system to the processing zone. The most optimal for the alloying were powders of spherical shape with a particle diameter of 50–120  $\mu\text{m}$ .

For supply and to be dosed powders into the processing zone, special devices have been developed and manufactured. (Figure 1).

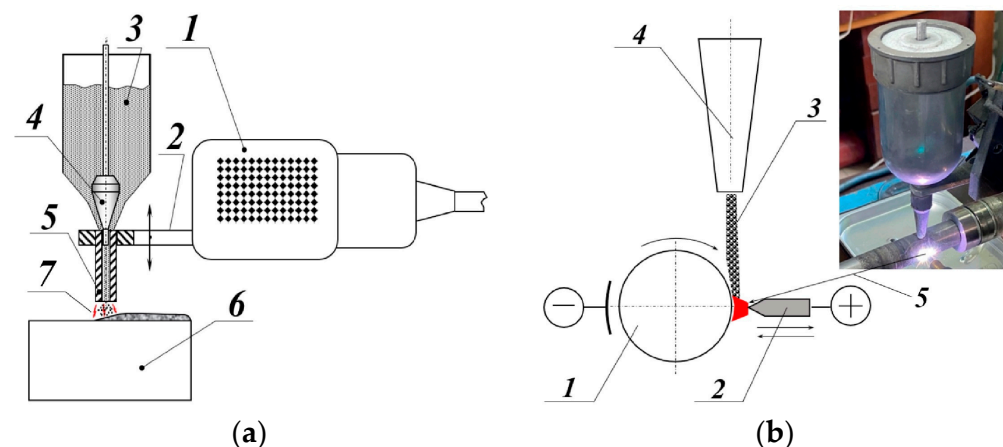


**Figure 1.** Schematic diagram of the technological methods of electrospark alloying with powder materials: (a) for flat surfaces (1—body; 2—anchor; 3—powder hopper; 4—jet; 5—hollow electrode; 6—substrate-cathode); 7—electrical discharge; (b) for cylindrical parts: (1—workpiece; 2—electrode-tool; 3—powder material; 4—powder hopper; 5—electrical discharge).

X-ray phase analysis of the obtained coatings was performed on a DRON-3.0 diffractometer (Bourestnik, JSC; Saint-Petersburg, Russia) in  $K\alpha$ —radiation with a tube with an anti-cathode made of copper, filtered at a wavelength of  $\alpha = 1.541 \text{ \AA}$ . The electrochemical behavior of the coatings was studied on a Multi Autolab M 204 potentiostat-galvanostat (Metrohm AG, Herisau, Switzerland). For corrosion testing, a 3% NaCl solution in distilled water was used as a background solution. The morphology of the coatings was studied

using an MDS 1600T optical metallographic microscope (Chongqing Optec Instrument Co., Ltd., Chongqing, China).

Sliding wear tests with the samples of steel C45 with coatings were carried out according to standard ASTM G77 with a block-on-roller friction machine equipped with a special device for recording the friction force. The test specimens were a parallelepiped with dimensions of  $5 \times 8 \times 6$  mm. The coating was applied to a surface with dimensions of  $5 \times 8$  mm. A roller of steel C45 (HRC 30) was used as a counter-body. The tests were carried out at a load of 2 MPa under dry friction conditions. The average speed value of counter-body movement was 0.075 m/s or 75 cycles per minute. The wear was assessed by the gravimetric method (according to the weight loss of the sample) using an electronic analytical balance. The total sliding distance was 1012.5 m.

X-ray phase analysis of the obtained coatings was performed on a DRON-3.0 diffractometer.

The electrochemical behavior of the coatings was studied on a Multi Autolab M 204 potentiostat-galvanostat (Metrohm AG, Herisau, Switzerland). For corrosion testing, a 3% NaCl solution in distilled water was used as a background solution.

The morphology of the coatings was studied using an MDS 1600T optical metallographic microscope.

### 3. Results

A comparison of the results of the traditional ESA using a compact electrode with the contact-powder method, proposed by us, convincingly showed that bringing the powders into the inter-electrode gap significantly increases the efficiency of the coating layers forming on a metal surface.

It is clear from Figure 2 that, other things being equal, in the case of using the powders of alloying materials, the formation of the coatings occurs much more intensively than in the case of ESA using a compact electrode.

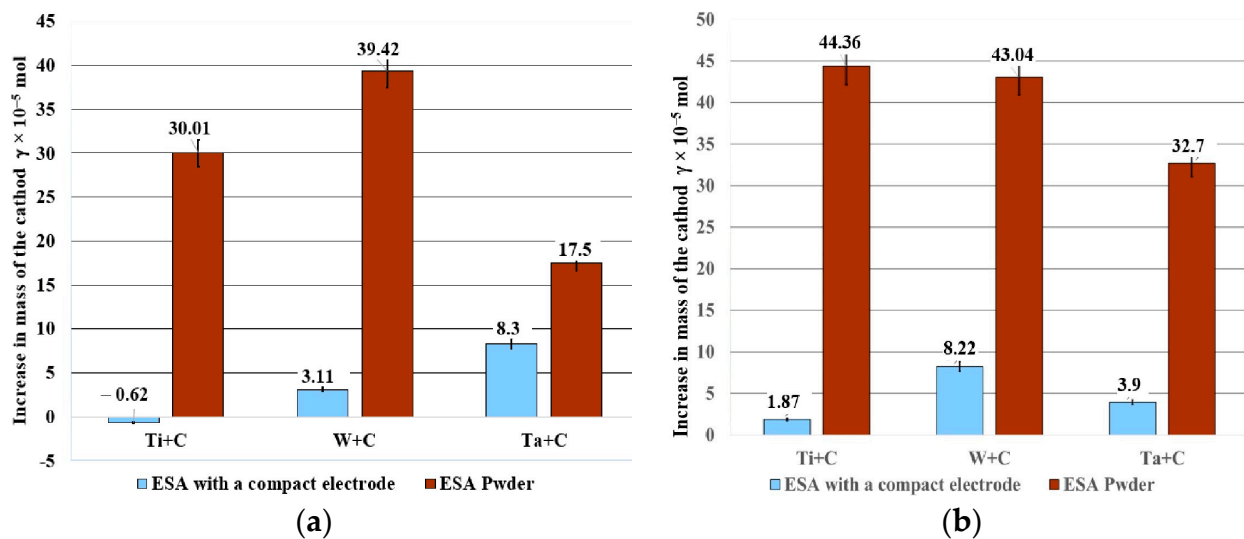


**Figure 2.** Histograms of cathode mass growth rates in the cases of ESA with compact and with additional supply of powder when the mode of the discharge energy was  $E_p = 0.3$  J: (a) cathode—C45, (b) cathode—commercial titanium BT1.

A similar picture is observed in the case of processing in the mode with the energy of pulsed discharges equal to  $E_p = 0.9$  J (Figure 3).

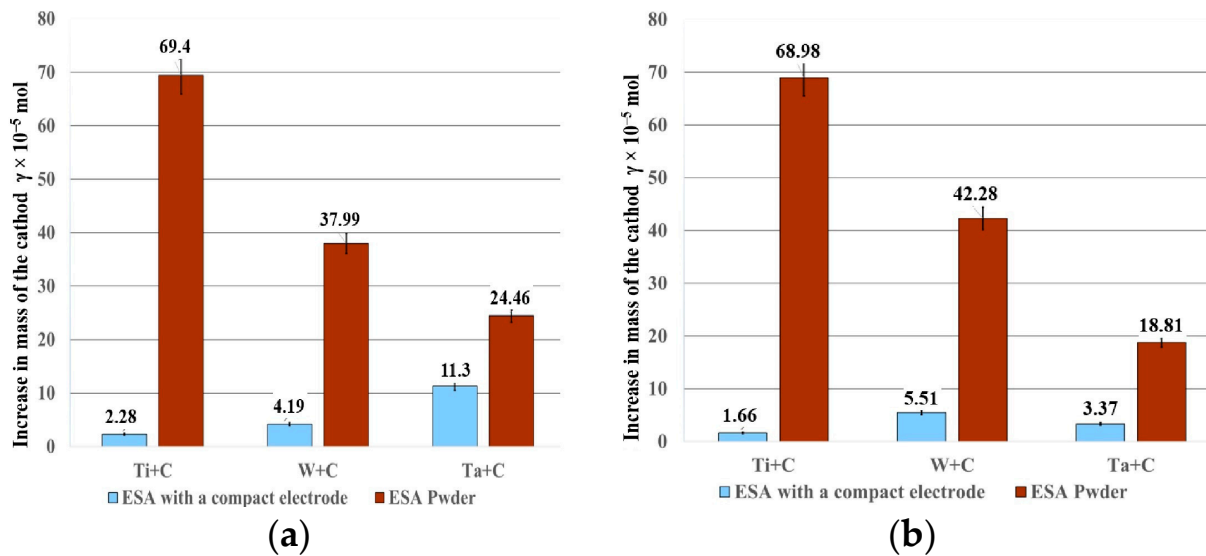


**Figure 3.** Histograms of cathode mass growth rates at the compact ESA and with additional powder supply when the mode of the discharge energy was  $E_p = 0.9$  J: (a) cathode—C45, (b) cathode—commercial titanium BT1.

As can be seen from the presented histograms, when powders were used as alloying materials, coatings were formed on the cathode in all cases, regardless of the different melting temperatures of the powder materials and the substrate (cathode). This indicates that the mechanism of formation of the coating layer on the cathode is somewhat different from the classical scheme of treatment with a compact electrode, which strictly obeys the polarity criteria ( $K_p$ ) of erosion according to B. Zolotykh [14] and L.S. Palatnik [15]:

$$K_p = \gamma_c / \gamma_a \quad (1)$$

where  $\gamma_c$  and  $\gamma_a$  are the cathode and anode erosion, respectively. This criterion puts forward the following conditions: if  $K_p < 1$ , then the polarity is positive and material transfer at the cathode will take place, and if  $K_p > 1$ , then the polarity is negative and there will be no transfer.

In the case of bringing a powder material into the zone of electrospark alloying, the transfer of material onto the cathode surface and the formation of a coating layer can be explained in terms of the behavior of a powder particle in a strong electric field. It is known [16] that when a powder particle gets between two electrodes that are under potential, the gap breakdown occurs at a distance greater than the standard discharge distance. As a result, a significant part of the thermal energy released as a result of the discharge, will be released in the inter-electrode gap, and much less energy will be released on the electrodes edges. Powder particles entering the discharge plasma channel melt and partially evaporate. In this form, the material of the particles is transferred onto the cathode by electric forces. Since the temperature of the cathode is less, when the liquid phase of the particle material enters, it cools down faster. Following the transfer of particles, the anode moves (electrode vibrates), reaches the surface of the cathode, and forges the coating material. At the same moment, a short-circuit current passes through the contact of the anode-particle-cathode, releasing additional heat which causes the intensification of micro-metallurgical processes in microvolumes.

The high-quality coatings obtained using the new version of ESA, with an additional powder material in the inter-electrode gap, showed a significant role of technological factors such as processing schemes and the state of aggregation of alloying elements (compact electrodes or powder materials), which will significantly expand the possibilities of the ESA method.

In that way, the fraction of energy used to process the powdered material is much larger, and therefore the intensity of the formation of the coating layer and its thickness on the cathode per unit of processing time is much greater (see Figures 2 and 3).

An analysis of the preliminary study results showed that the use of powder materials for coating by the electrospark alloying process disclosed new possibilities of the method in terms of creating multicomponent layers using various materials and their mixtures.

It has been experimentally estimated that to obtain good-quality layers with carbide phases, similar to those obtained with compact electrodes ESA, the discharge energy must be increased by 1.3–1.5 times. During ESA, with compact electrodes made of graphite and titanium, high-quality layers were obtained in modes with a discharge energy of  $W_p = 1.0$  J. In the case of additional powder supplies of these materials into the inter-electrode gap, the energy must be increased to 2.5–3.0 J. Processing at optimal conditions made it possible to obtain homogenous coatings with a hardness of 3.5–4.5 times greater than that of the steel base. Figures 4 and 5 show a micrograph of a sample of C45 steel coated by ESA with a mixture of titanium and graphite powders fed into the interelectrode gap.

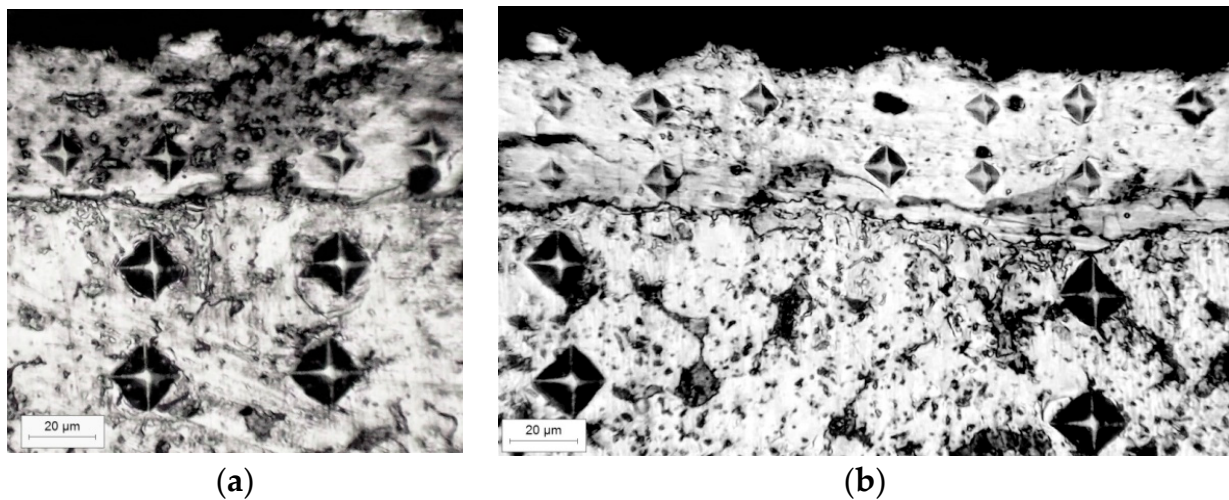


**Figure 4.** Microstructure of the coating on steel C45, obtained by ESD with the supply of a mixture of titanium and graphite powders to the MEP: (a) discharge energy  $E_p = 0.3$  J and (b) discharge energy  $E_p = 0.9$  J.

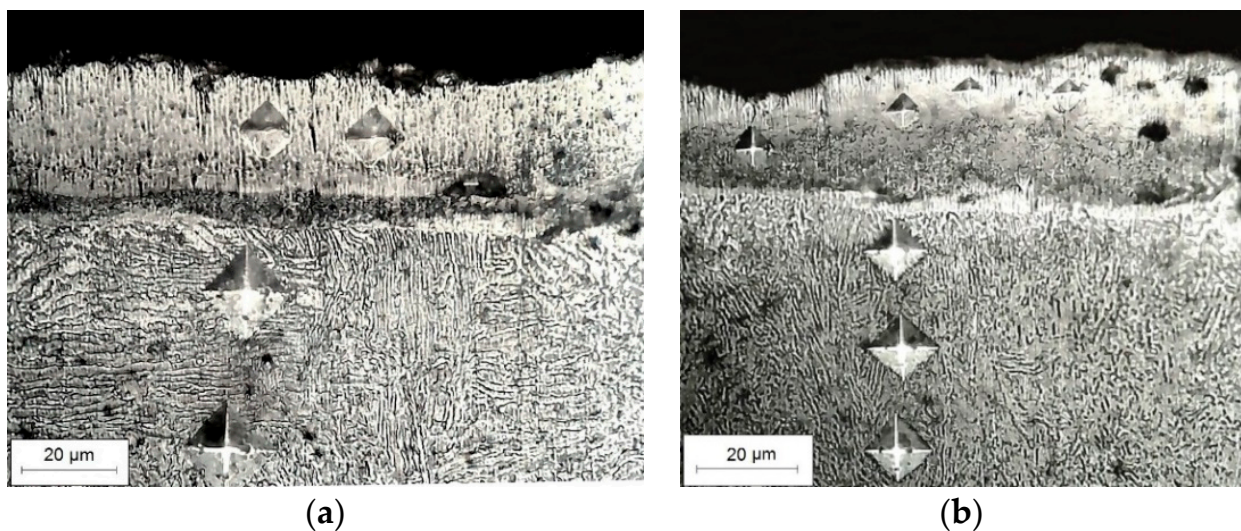


**Figure 5.** Microstructure of titanium alloy OT4 subjected to ESD with a mixture of powders of tungsten and graphite (a), and molybdenum and graphite (b).

Similar coatings on titanium substrate were obtained during ESA with a mixture of powders from tantalum and graphite (Figure 5), as well as from molybdenum and graphite and from tungsten and graphite, which are characterized by a rather high density, thickness uniformity, and high uniformity.

An important factor in case of ESA with the powder supply is the powder grain size. Experiments were carried out with particle sizes ranging from 5 to 200  $\mu\text{m}$ .

When using fine-dispersed powders up to sizes of 70–80 microns, the process of coating formation is quite complicated. Poor flow ability and strong clumping were observed. As the granularity increases, these negative phenomena decrease, and when the particle size was 120–200  $\mu\text{m}$ , the process stabilizes since it becomes possible to uniformly dose the amount of powder supply into the inter-electrode gap.

The high microhardness of the coatings formed upon the introduction of powder materials into the inter-electrode gap indicates their intense interaction with the spark discharge plasma and the substrate material, followed by the formation of various compounds.

X-ray analysis of coatings on steel samples in cobalt  $K\alpha$  radiation and on titanium samples in copper  $K\alpha$  radiation showed the presence of carbides of the corresponding metals. For example, during electrospark alloying of a steel sample with a titanium electrode and then with a graphite electrode, titanium carbide and free carbon, as well as a small amount of  $\text{TiO}_2$ , were found in the layers.

After the ESA with tungsten and then with graphite electrodes, two modifications of tungsten carbide, WC and  $\text{W}_2\text{C}$ , as well as free graphite, were found in the surface layers.

Figure 6 shows the diffraction patterns obtained from the surface of a titanium sample processed in modes with values of the discharge energy:  $W_p = 0.3 \text{ J}$ ;  $W_{p1} = 1.0 \text{ J}$ .

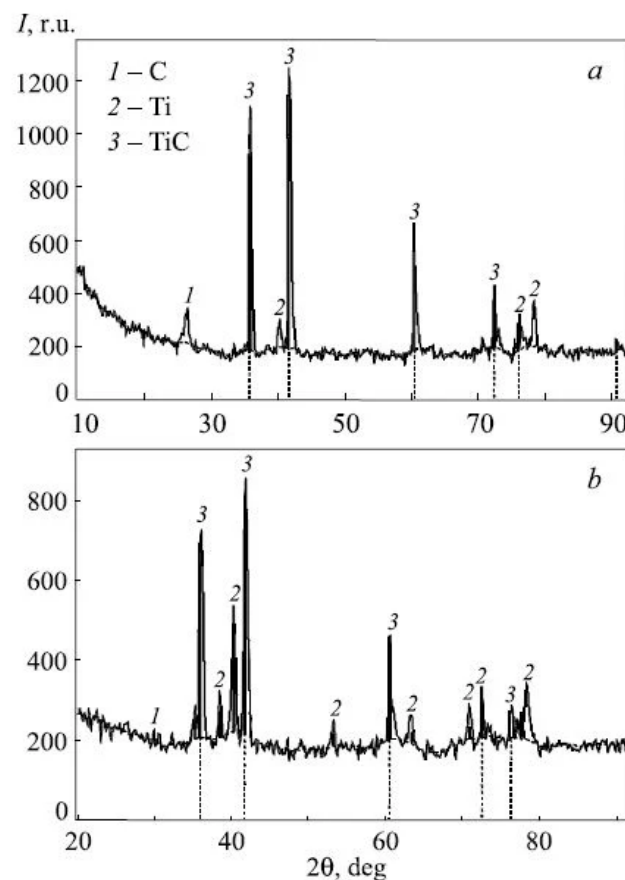


**Figure 6.** Diffraction patterns obtained from the surface of Ti samples subjected to ESA with a graphite electrode in different modes ( $W$ ): (a)  $W = 0.3 \text{ J}$ ; (b)  $W = 1.0 \text{ J}$  [6].

As can be seen, in both cases, a carbide phase (TiC) arises, with the only difference being that in the mode with a lower energy of electrical pulses, the amount of free graphite is much greater. At higher discharge energies, the interaction of titanium with graphite (carbon) is more intense and free carbon remains less.

A similar picture was also obtained during the sequential processing of Cr18Ni10T austenitic steel with tungsten and graphite electrodes.

The former measurements estimated that initial microhardness value of Cr18Ni10T steel at the load of 50 g was  $3.23 \pm 0.26$  GP and after electrospark deposition of W + graphite surface hardness increased up to  $15.20 \pm 1.29$  GPa. After depositing with Mo + graphite it varied  $4.02 \pm 0.41$ – $14.38 \pm 1.1$  GPa. Minimal microhardness was at bottom layers of coating, and maximum—at the top layers. The measurement of the microhardness of the obtained coatings showed an increase of 3.5–4.7 times, which confirms the presence of carbide phases in the coatings as well as nitrides because the treatment was carried out in air [17].

### 3.1. Synthesis of Ternary Compounds (MAX-Phases)

Ternary compounds (MAX-phases) are a family of ternary layered compounds with a formal stoichiometry of  $M_n + 1 AX_n$  ( $n = 1, 2, 3, \dots$ ), where M is a transition d-metal; A is a p element (for example, Si, Ge, Al, S, Sn, etc.); and X is a carbon or nitrogen [18–22].

Layered triple carbides and nitrides of d- and p-elements (MAX-phases) exhibit a unique combination of properties characteristic of both metals and ceramics. Such materials have a low density, high values of thermal and electrical conductivity, strength, a low modulus of elasticity, excellent corrosion resistance in aggressive liquid media, resistance to high-temperature oxidation and thermal shock, are easily machined, have a high melting point, and are quite stable at temperatures up to 1000 °C and higher [18].

Among the many MAX phases synthesized to date, those of greatest interest in terms of the level of their properties are MAX phases based on titanium:  $Ti_2AlC$ ,  $Ti_2AlN$ ,  $Ti_3AlC_2$ ,  $Ti_3SiC_2$ . The synthesis of such compounds is achieved by hot isostatic pressing, plasma discharge sintering (PDS), and SHS.

These industrial processes are associated with the use of complex and expensive equipment with high energy costs. In this regard, of interest is the synthesis and application of such MAX-phases as hardening coatings on the working surfaces of machine parts using, for these purposes, less energy-intensive technologies such as, for example, electrospark metal surface alloying, which has a number of advantages, including low energy and material consumption, simplicity of the process, and equipment for its implementation.

To obtain MAX phases by electrospark alloying on structural steel C45 and the titanium alloy VT6, we used three technological methods [6]. In the first case, compact electrodes were used from those elements (materials) that are part of the MAX phases. For example, to obtain a MAX phase consisting of Ti, Al, and C, the sample was sequentially coated with titanium, aluminum, and then graphite at different energy modes and treatment times per area unit in order to determine the optimal conditions for obtaining ternary compounds.

According to another processing scheme, when powders of the same materials were used as alloying elements, it became possible to ensure the stoichiometric composition of powder mixtures. Thus, the ESA process was carried out using mixtures of formal stoichiometry for the following compositions:  $TiAlC$ ,  $TiAlN$ ,  $TiSiC$ , in order to eventually obtain the MAX phases:  $Ti_2AlC$ ,  $Ti_2AlN$ ,  $Ti_3SiC$ .

The results of the X-ray phase analysis showed that the MAX-phases in the coatings are formed in modes with an energy of electrical pulsed discharges of 1.0–3.0 J. The diagram shown in Figure 7 confirms the formation of the  $Ti_3AlC_2$  MAX-phase.

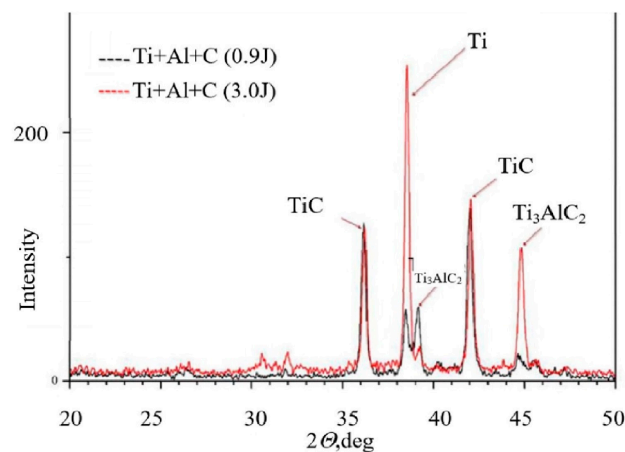


**Figure 7.** X-ray diffraction pattern of the coating on Cr18Ni10T steel, obtained by successive treatment with titanium, aluminum, and graphite electrodes and their powders.

Similar results were also obtained in sequential electrospark treatment with titanium electrodes and AlN and SiC powders.

Metallographic analysis of cross sections of samples with coatings obtained by sequential processing of technical titanium BT1 with electrodes made of titanium, aluminum, and graphite in the mode of electrode vibration and with varying the discharge energy in the range of 0.3–3.0 J showed that, regardless of the value of the electrical impulse energy of the processing, the formed layers are characterized by low continuity, uniformity in thickness, and quality (Figure 8a). While processing in the same energy modes with rotating wire electrodes, uniform thickness and continuous coatings of good quality were obtained (see Figure 8b).

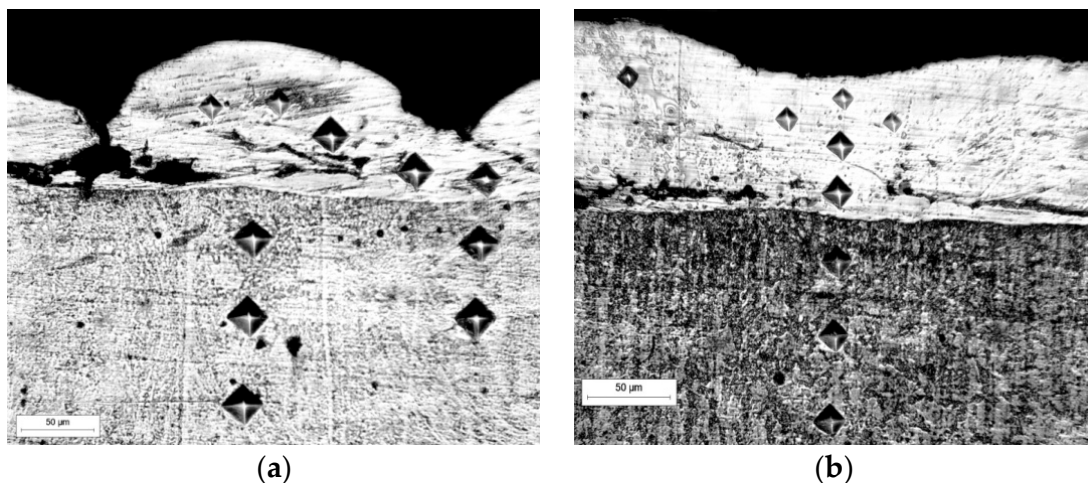


**Figure 8.** The structure of samples from steel C45 with TiAlC coatings, obtained by successive processing with electrodes from Ti, Al, and graphite in a vibrating mode (a) and with rotating wire electrodes in a plane perpendicular to the cathode surface (b).

According to another processing scheme, powders of the same materials (titanium, aluminum, graphite, TiN, SiC) were used as alloying elements, which were supplied into the inter-electrode gap during the ESA process. In this case, it became possible to ensure the stoichiometric composition of powder mixtures.

In the compact-powder variant of alloying, a wire of these metals with a diameter of 1.5–2.0 mm was used as processing electrodes made of titanium and aluminum (which are plastic metals), and silicon carbide SiC and titanium nitride TiN were used in the powder form. The formation of the coating was carried out as follows: A coating was applied to

the substrate using aluminum or titanium wire electrodes rotating in a plane perpendicular to the treated surface, and then, at the next stage, treatment with TiN or SiC powders was carried out.

Metallographic analysis of sample cross-sections with coatings obtained by sequential processing of C45 steel with titanium, aluminum, and graphite electrodes in the mode of electrode vibration and with varying the discharge energy in the range of 0.3–3.0 J showed that, regardless of the electric pulse energy value of processing, the formed layers are characterized by low continuity and uniformity in thickness (Figure 9a), while when processing in the same energy modes with a “turntable” applicator, good quality uniform and continuous coatings were obtained (see Figure 9b).

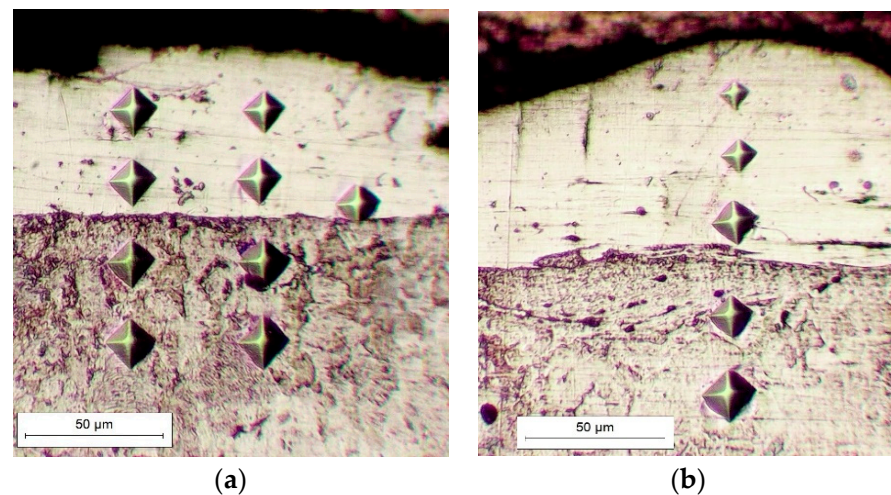


**Figure 9.** Micrographs of St.45 steel samples with 3-component TiAlN (a) and TiSiC (b) coatings.

### 3.2. Evaluation of the Tribological Characteristics of Coatings on Steel C45 Obtained by ESA with TiAlC, TiAlN, and TiSiC Compositions

Tribological tests were used to evaluate the wear resistance efficiency of the obtained coatings. The results are presented by the wear curves (Figure 10).

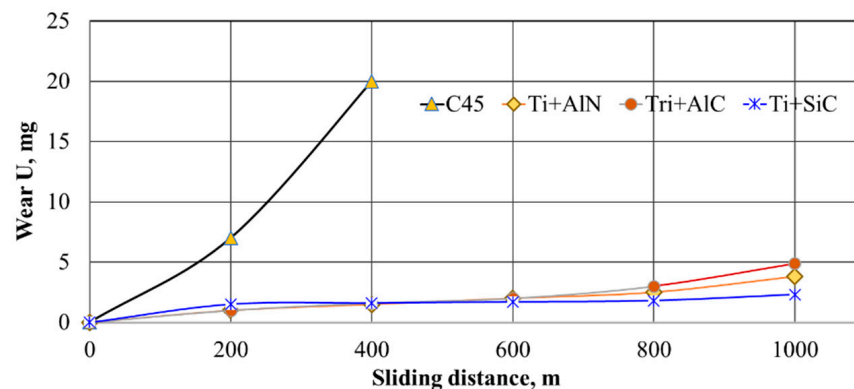


**Figure 10.** Coating wear at a specific load of 2 MPa.

As can be seen from the graph (Figure 10), all obtained coatings showed a much higher wear resistance compared to steel C45 without coating. The difference in wear resistance of coated samples is not significant, but the ternary-layered Ti+Si+C compound has higher wear resistance compared to the Ti+Al+N compound. That could be related to the higher hardness of compounds with higher Si and C content and the formation of hard carbides.

### 3.3. Corrosion Behavior of ESA Synthesized Coatings

Samples of stainless (medical) steel grade 40Cr13 were chosen as objects for research. Rods made of titanium, tungsten, MPG-6 graphite, silicon carbide (SiC), and aluminum nitride (AlN) with dimensions of  $40 \times 5 \times 5$  mm were used as anodes (processing electrodes). Coatings were deposited by two technological methods: by successive processing with compact electrodes of the indicated materials and by supplying powder mixtures of the same materials into the inter-electrode gap. The optimal grain size of the applied powder materials was 80–120  $\mu\text{m}$ . Before corrosion testing, some characteristics of the surface layers were studied, such as surface morphology, continuity, thickness uniformity, and microhardness.

Based on the conducted studies, it was found that coatings obtained as a result of successive treatment with electrodes made of graphite and titanium, as well as graphite and tungsten, have the highest corrosion resistance. It is confirmed by the polarization curves of electrospark coatings [23] and corrosion current values (Figure 11).

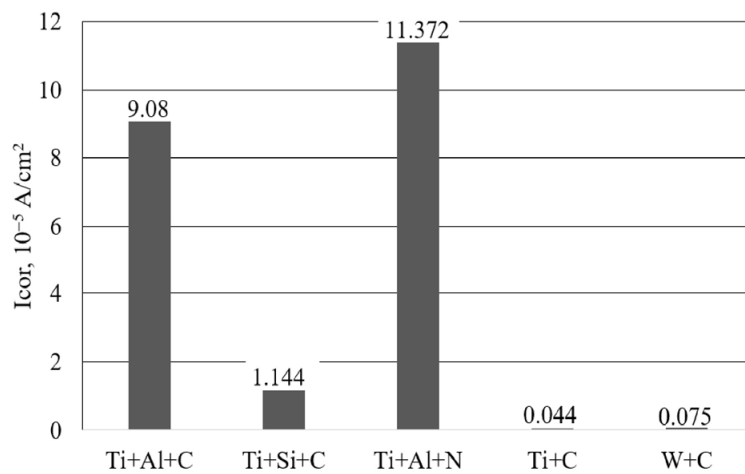


**Figure 11.** Corrosion current values for various electrospark coatings at current density  $10^{-5}$  A/cm $^2$ .

The results show that coatings retain their original morphology after exposure to a corrosive environment and show high corrosive resistance.

The three-component coatings, Ti+Al+C, Ti+Si+C, and Ti+Al+N, were less resistant in an aggressive environment (Figure 11f). This can be explained by the fact that when processing with compact electrodes, such elements as aluminum, under otherwise equal conditions, are transferred to the cathode in a larger amount in one act of discharge, and a layer of considerable thickness is formed during the optimal processing time, which is a kind of barrier to the penetration of carbon and filling defects in the form of pores, microcracks, etc.

The studies conducted to determine the physical and mechanical characteristics of coatings after corrosion tests showed that the microhardness values for Ti+C and W+C do not actually change (Table 1), which indicates that they were not subjected to electrochemical dissolution. For specimens with Ti+Al+C, Ti+Si+C, and Ti+Al+N coatings, a decrease in microhardness values by 16%–19% is observed compared to the initial values before corrosion tests.

**Table 1.** The value of the microhardness of coatings formed on steel 40Cr13 after corrosion.

Microhardness of Coatings	Coating Composition					
	40Cr13	Ti+Al+C	Ti+Si+C	Ti+Al+N	Ti+C	W+C
N, GPa	$4.7 \pm 0.44$	$5.2 \pm 0.54$	$8.9 \pm 0.51$	$9.8 \pm 0.8$	$13.4 \pm 1.28$	$15.7 \pm 1.34$

#### 4. Discussion

According to the established concepts [6], electrospark coatings are formed as a result of the intense interaction of pulsed discharge plasma with anode and cathode materials. Formation of various alloys, pseudo-alloys, nitrides, and oxides takes place if processing in the air, and diffuse penetration of coating materials proceeds into the base. Former research [6] has shown that during sequential treatment with graphite and any transition metals of IV-VI groups of the periodic system, the carbides of the corresponding metals are formed in the surface layers. As a result of such treatment, the hardness and wear resistance of the formed layers significantly increase [24]. That is also confirmed by our wear resistance results (Figure 10).

The morphology of this particular surface layer is an “island” structure. Coalescence of these structures is possible with the formation of a continuous film, the number of defects in which depends on the technological modes of processing and the chemical composition of the electrodes. There is a layer formed underneath as a result of diffusion penetration of the anode and cathode materials. The microhardness of this zone is somewhat lower than that of the upper layer. The existence of an upper hard layer and a diffusion zone, which also has a sufficiently high hardness in comparison with the hardness of uncoated steel 40Cr13, ultimately ensures a long service life of the coating.

High local temperatures during electrospark alloying lead to the formation of a fairly wide layer, the structure of which is characterized by a crystalline structure that differs from the structure of the modified material. Typically, this layer is characterized by a fine-dispersed structure. With an increase in the depth of the modified layer, a gradual transition of this fine-dispersed component into the structure of the base material grain size is observed [6]. An interesting feature of the formation of electrospark coatings upon successive treatment with one of the transition metals and graphite should be noted. Despite the fact that the ESA process is discrete, the coatings are formed as a result of the transfer of individual portions of the anode material to the surface of the cathode (workpiece), and, as a result, it is impossible to obtain layers of 100% wholeness. At the same time, in our case, we obtained extremely high corrosion resistance of the 40Cr13 steel specimens subjected to successive electrospark alloying with electrodes made of titanium and graphite, or of tungsten and graphite. This can be explained by the fact that during the electrical erosion of graphite, the polar transfer to the cathode occurs in the form of ions and carbon atoms, as well as fine particles of graphite [24]. The presence of this flow and the liquid phase of the cathode material, which occur when the discharge plasma acts on the electrode surface, leads to the diffusion and interaction of carbon with the materials of the liquid and solid phases of the substrate and the mechanical mixing of solid particles of graphite and liquid.

Since the ejection of graphite particles continues even after the completion of the discharge [24], a layer of fine-dispersed graphite particles is formed on the cathode surface, especially at the beginning of the treatment process, some of which penetrates into the crystallizing melt and also fills in the dimples of the irregularities of the forming surface. Hereby, as a result of such processing, a dense, impermeable layer for an aggressive liquid is formed.

#### 5. Conclusions

1. The process has been developed for the formation of multicomponent coatings with electrospark alloying using the supply of powder materials into the inter-electrode gap.
2. Under the same energy regimes and processing times, the supply of powder material to the electrospark alloying zone contributes to an increase in coating formation intensity on the cathode substrate of 10 or more times compared with the classical process with a compact electrode.
3. The highest quality coatings of the developed ESA method are received at the energy of the electric pulsed discharge in the range of 0.8–3.0 J.

4. It is suggested that the ESA method can expand the range of materials used for alloying and could be used for synthesizing MAX-phase coatings, which have unique properties for both metals and ceramics.
5. At the interaction of the plasma of pulsed discharges and powder and substrate materials, the nanocrystalline and amorphous phases are formed in surface layers.
6. Sliding wear tests of structural steel C45 with coatings of TiAlC, TiAlN, and TiSiC compositions show a decrease in wear by an average of 6 times compared to uncoated steel.
7. The substrate of 40X13 steel coated with TiC and WC has high corrosion resistance in a 3% NaCl solution. The corrosion current of these coatings is 0.044 and 0.075 A/cm<sup>2</sup>, respectively, and is significantly less than that of the non-coated substrate.

**Author Contributions:** Conceptualization, V.M. and R.R.; methodology, E.O. and N.K.; validation, V.M., N.K., S.I., E.O., A.I., R.R. and A.Z.; formal analysis, V.M. and N.K.; investigation, N.K., E.O. and C.B.; data curation, V.M., E.O., C.B. and A.I.; writing—original draft preparation, V.M. and R.R.; writing—review and editing, A.Z.; supervision, V.M. and R.R.; funding acquisition, V.M. All authors have read and agreed to the published version of the manuscript.

**Funding:** This research was funded by the H2020-MSCA-RISE project SMARTELECTRODES (Grant No. 778357) and ANCD project 22.80013.5007.7BL (2022–2023) “Technology and equipment for the deposition of multicomponent and multifunctional coatings on metal surfaces at the interaction of the plasma of low-voltage impulse discharges with powdery materials”.

**Institutional Review Board Statement:** Not applicable.

**Informed Consent Statement:** Not applicable.

**Data Availability Statement:** Not applicable.

**Conflicts of Interest:** The authors declare no conflict of interest.

## References

1. Sauszkin, B.P. *Fiziko-Chimicheskie Metody Obrabotki v Proizvodstve Gazoturninykh Dvigatelyei*; Drofa: Moscow, Russia, 2002; p. 655.
2. Bologa, M.K. Jurnal nastoiashego i budeshhego –Elektronnaya Obrabotka Materialov” —55 let (Journal of the Present and the Future—“Elektronnaya Obrabotka Materialov” —55 years old). *EOM* **2020**, *56*, 1–13. [[CrossRef](#)]
3. Ivanov, V.I.; Burumkulov, F.C. Uprochnenie i uvelichenie resursa objektiv elektroiskrovym metodom: Klafifikacija, ossobenosti tehnologii. *Electr. Surf. Treat. Methods* **2010**, *46*, 27–36.
4. Michailiuk, A.I.; Gitlecich, A.E. Primenenie grafita v elektroiskrovych tehnologiach. *Electr. Surf. Treat. Methods* **2010**, *5*, 37–44.
5. Katinas, E.; Jankauskas, V.; Kazak, N.; Mikhailov, V. Improving Abrasive Wear Resistance for Steel Hardox 400 by Electro-Spark Deposition. *J. Frict. Wear* **2019**, *40*, 100–106, ISSN 1068-3666. [[CrossRef](#)]
6. Mikhailov, V.V.; Kazak, N.N.; Agafii, V.I.; Yanakevich, A.I. Synthesis of Carbide Phases in Surface Metal Layers Under Electrospark Alloying with Graphite and Transition Metals in Groups IV–VI. *Powder Metall. Met. C* **2019**, *58*, 307–311, ISSN 1068-1302. [[CrossRef](#)]
7. Penyashki, T.G.; Radev, D.D.; Kandeveva, M.K.; Kostadinov, G. Structural and Tribological Properties of Multicomponent Coatings on 45 and 210Cr12 Steels Obtained by Electrospark Deposition with WC-B4C-TiB<sub>2</sub>-Ni-Cr-Co-B-Si Electrodes. *Surf. Eng. Appl. Electrochem.* **2019**, *55*, 638–650. [[CrossRef](#)]
8. Lu, K.; Zhu, J.; Ge, W.; Hui, X. Progress on New Preparation Methods, Microstructures, and Protective Properties of High-Entropy Alloy Coatings. *Coatings* **2022**, *12*, 1472. [[CrossRef](#)]
9. Barile, C.; Casavola, C.; Pappalè, G.; Renna, G. Advancements in Electrospark Deposition (ESD) Technique: A Short Review. *Coatings* **2022**, *12*, 1536. [[CrossRef](#)]
10. Nikolenko, S.V.; Verkhoturov, A.D. *Novyye Elektrodnyye Materialy Dlya Elektroiskrovogo Legirovaniya*; Vladivostok Dal’nauka: Vladivostok, Russia, 2005; p. 219.
11. Kazak, N. Sintetizarea prin electroeroziune a carburilor pe suprafețele metalice. *Akademios* **2019**, *2*, 31–34, ISSN 1857-0461. [[CrossRef](#)]
12. Opong Boakyee, G.; Geambazu, L.E.; Ormsdottir, A.M.; Gunnarsson, B.G.; Csaki, I.; Fanicchia, F.; Kovalov, D.; Karlsdottir, S.N. Microstructural Properties and Wear Resistance of Fe-Cr-Co-Ni-Mo-Based High Entropy Alloy Coatings Deposited with Different Coating Techniques. *Appl. Sci.* **2022**, *12*, 3156. [[CrossRef](#)]
13. Mehmood, K.; Umer, M.A.; Munawar, A.U.; Imran, M.; Shahid, M.; Ilyas, M.; Firdous, R.; Kousar, H.; Usman, M. Microstructure and Corrosion Behavior of Atmospheric Plasma Sprayed NiCoCrAlFe High Entropy Alloy Coating. *Materials* **2022**, *15*, 1486. [[CrossRef](#)] [[PubMed](#)]

14. Zolotykh, B.N.; Gioev, K.K.H. O roli mekhanicheskikh faktorov v protsesse erozii v impulsnom razryade. In *Fizicheskiye osnovy elektroiskrovooy obrabotki materialov*; Nauka: Moscow, Russia, 1966; pp. 16–31.
15. Palatnik, A.S. *Izvestiya ANSSR, seriya fizicheskaya*; MGU: Moscow, Russia, 1951; p. 80.
16. Mesyats, G.A. *Vzryvnaya Elektronnaya Emissiya*; Izdatel'stvo "Fizmatlit": Moscow, Russia, 2016; p. 273.
17. Kukareko, V.; Agafii, V.; Mihailov, V.; Grigorich, A.; Kazak, N. Evaluation of Tribological Properties of Hard Coatings Obtained on Steel C45 by Electro-spark Alloying. *Key Eng. Mater.* **2019**, *813*, 381–386, ISSN 1662-9795. [[CrossRef](#)]
18. Barsoum, M.W.; El-Raghy, T. Processing and Mechanical Properties of Ti<sub>3</sub>SiC<sub>2</sub>:1. Reaction Path and Microstructure Evaluation. *J. Am. Ceram. Soc.* **1999**, *82*, 2849–2854.
19. Barsoum, M.W.; Ali, M.; El-Raghy, T. Processing and Characterization of Ti<sub>2</sub>AlC, Ti<sub>2</sub>AlN, Ti<sub>2</sub>AlC. *Metall. Mater. Trans.* **2000**, *31*, 1857–1865. [[CrossRef](#)]
20. Yan, M.; Mei, B.; Zhu, J.; Tian, C.; Wang, P. Synthesis of High-Purity Bulk TiAl<sub>2</sub>N By Spark Plasma Sintering (SPS). *Ceram. Int.* **2008**, *34*, 1439–14427. [[CrossRef](#)]
21. Naguib, M.; Kurtoglu, M.; Presser, V.; Lu, J.; Niu, J.; Heon, M. Dimensional Nanocrystals Produced By Exfoliation of Ti<sub>3</sub>AlC<sub>2</sub>. *Adv. Mater.* **2011**, *23*, 4248–4253. [[CrossRef](#)] [[PubMed](#)]
22. Smetkin, A.A.; Mayorova, Y.K. Svoystva Materialov Na Osnove MAX-Faz. Vestnik PNIPU, Mashinostroyeniye. *Materialovedeniye* **2015**, *17*, 120–138.
23. Kazak, N.N.; Mikhaylov, V.V.; Chekan, N.M.; Ovchinnikov, Y.V.; Eysymont, Y.I.; Kovsh, A.A. Korroziionnaya stoykost' i prochnostnyye kharakteristiki nanostrukturirovannykh pokrytiy, poluchennykh metodom elektroiskrovogo legirovaniya. In Proceedings of the International Conference Actual Strength Issues, Vitebsk, Belarus, 25–29 May 2020; pp. 320–322, ISBN 978-985-6967-44-6.
24. Mitskevich, M.K.; Bushik, A.I.; Bakuto, I.A.; Shilov, V.A. Izucheniye Dinamiki Protsessa Perenosa Materiala Elektroodov V Silnotochnom Impulsnom Razryade. *Elektron. Obrab. Mater.* **1977**, 18–19.

**Disclaimer/Publisher's Note:** The statements, opinions and data contained in all publications are solely those of the individual author(s) and contributor(s) and not of MDPI and/or the editor(s). MDPI and/or the editor(s) disclaim responsibility for any injury to people or property resulting from any ideas, methods, instructions or products referred to in the content.